

## A USNCTAM Report on Recent Trends in Mechanics

### RESEARCH TRENDS IN BIOLOGICAL FLUID DYNAMICS

Sunghwan (Sunny) Jung<sup>†</sup>, Virginia Tech; [sunnjsh@vt.edu](mailto:sunnjsh@vt.edu)

Anne E. Staples<sup>†</sup>, Virginia Tech; [aestaples@vt.edu](mailto:aestaples@vt.edu)

John O. Dabiri, Stanford University; [jodabiri@stanford.edu](mailto:jodabiri@stanford.edu)

Alison L. Marsden, Stanford University; [amarsden@stanford.edu](mailto:amarsden@stanford.edu)

Manu Prakash, Stanford University; [manup@stanford.edu](mailto:manup@stanford.edu)

Kristen A. Davis, University of California, Irvine; [davis@uci.edu](mailto:davis@uci.edu)

Shawn C. Shadden, University of California, Berkeley; [shadden@berkeley.edu](mailto:shadden@berkeley.edu)

Thierry Savin, University of Cambridge; [t.savin@eng.cam.ac.uk](mailto:t.savin@eng.cam.ac.uk)

Lydia Bourouiba, Massachusetts Institute of Technology; [lbouro@mit.edu](mailto:lbouro@mit.edu)

Josué Sznitman, Technion – Israel Institute of Technology; [sznitman@bm.technion.ac.il](mailto:sznitman@bm.technion.ac.il)

<sup>†</sup>Corresponding authors, emails: [sunnyjsh@vt.edu](mailto:sunnyjsh@vt.edu) and [aestaples@vt.edu](mailto:aestaples@vt.edu)

### Introduction

Biological fluid dynamics is arguably one of the most active, visible, and exciting areas of fluid dynamics research today, with studies in areas ranging from the human cardiovascular system to marine animal propulsion. The aim of this article is to summarize emerging trends in biological fluid dynamics, and to identify core areas of interest, and future directions at the intersection of fluid dynamics and other, adjacent fields such as biology and medicine that are of critical technical and societal importance. On September 15-16, 2014 the Workshop on Fluid Dynamics of Living Systems was held in Arlington, Virginia, with NSF support. Contributors to this article were selected among the invited speakers to the workshop. This research trend article is intended to bring attention to critical, emerging directions in biological fluid dynamics, and also to provide students and researchers who were not able to attend the workshop with a summary of the major research discussed by experts in the field.

The report focuses on five core areas of research, 1) the fluid dynamics of benthic coastal systems, which links many of the physical and biological processes in coastal communities and is crucial to understand in the face of a changing climate; 2) image-based hemodynamics modeling, which allows for patient-specific, personalized models of vascular blood flow, an important direction in medicine; 3) blood occlusions in the microcirculation. The microvascular network is central in certain pathological conditions such as anemia and tumor-induced angiogenesis and, as imaging techniques improve, it is possible to study the microcirculation in new ways; 4) the fluid dynamics of disease transmission. Considering localized fluid flows of epidemiological interest from a novel, fundamental mechanics perspective can uncover factors important for public health, as well as of interest to the general fluid dynamics community; 5)

respiratory flows in the deep pulmonary airways. The fluid mechanics of the acinar region of the lung, which is made of hundreds of millions of sub-millimeter gas-exchange units (alveoli), is a field where many new advances are being made which have the potential to remove the need for animal testing in the study of inhaled aerosols in the lungs.

## 1. Fluid dynamics of coastal benthic ecosystems by Kristen A. Davis

Hydrodynamics plays an important role in benthic communities in the coastal ocean. Fluid flow controls the transport and mixing of biologically important material and regulates ecosystem functions such as photosynthesis, nutrient uptake, and benthic grazing. Understanding the links between physical and biological processes in coastal communities is increasingly important as we try to predict the resilience of these communities in the face of a changing climate.

One of the coastal communities most impacted by the changing climate is coral reefs. Ocean acidification is projected to reduce calcification on reefs 10-50 % by the end of the century [1] – threatening to erode the building blocks of reef ecosystems. Rising sea surface temperatures are a severe threat to reefs, as tropical corals are widely thought to live near their upper thermal limits [2]. Heat stress can lead to the breakdown of symbiosis between the coral animals and their endodermal symbiotic algae, resulting in the loss of pigmentation, or “bleaching”, and can lead to mortality [3]. The National Oceanic and Atmospheric Administration recently designated the year 2015 as the third global bleaching event for corals (the first two being in 1998 and 2010). But we have many unanswered questions about the role of fluid dynamics in the ecosystem function of reefs.

### *Hydrodynamic Controls on Benthic-Pelagic Coupling*

The geometric complexity of coral reefs leads to interesting fluid dynamics questions at scales of individual coral polyps to the scales of the carbonate platform or island on which they grow [4]. One of the most obvious features of coral reefs is that they are rough, having effective bottom drag coefficients that are typically an order of magnitude larger than the canonical value found over muddy or sandy sea beds. These large roughness elements are very effective at generating turbulent mixing and, combined with a high surface area, maximize mass transfer between the coral and the surrounding water. The geometric complexity of reefs makes it challenging to predict the drag and resultant boundary layer flow profile over reefs. For example, in geophysical boundary layers, the commonly used law-of-the-wall is

$$u(z) = \frac{u_*}{\kappa} \ln\left(\frac{30z}{k_s}\right) \quad (1)$$

where  $u_*$  is the friction velocity (essentially shear stress in velocity units),  $\kappa = 0.41$  is the von Karman constant,  $z$  is the height above the bed, and  $k_s$  is an equivalent sand grain roughness. However the complex morphology of reefs does not lend itself well to characterization using a

single length scale ( $k_s$ ) and concepts from urban canopy flow [5,6] and porous media flow [7], have proven more successful at predicting drag and boundary layer flows over rough reef beds.

Studies of nutrient uptake rates on reef benthic communities by Marlin Atkinson and several others have shown that nutrient uptake on coral reefs is “mass transfer limited”, or limited by flux across a thin boundary layer which covers the surface of the organism [8]. Thus, the rate at which benthic reef organisms exchange material with the water column is dependent upon flow conditions and the concentration of the material near the bed. A consequence of this flow-dependence is that the removal of nutrients by benthic organisms leads to a region of depleted nutrient or phytoplankton concentration near the bed or a “concentration boundary layer. The concentration boundary layer represents a balance between the removal rate of material near the bed and the replacement of that material through downward turbulent mixing. The observation of concentration boundary layers existing in natural reef settings (e.g. ref. [9]) highlights the important role of boundary layer turbulence in reef ecosystem functions.

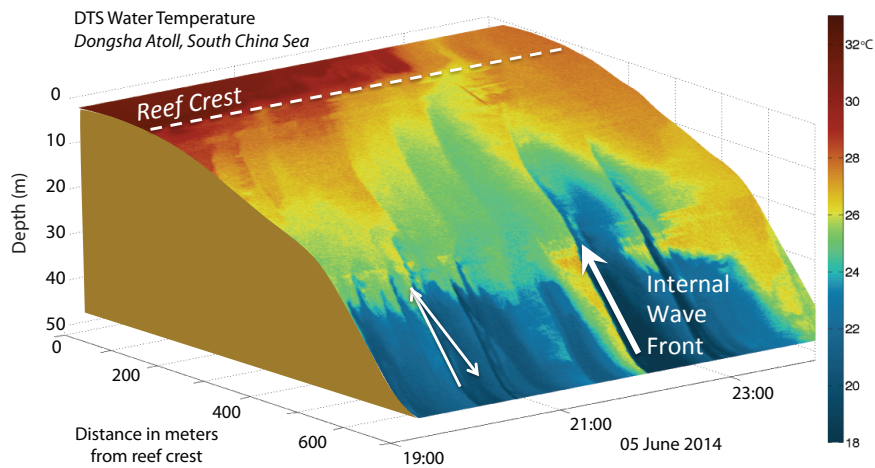


Figure 1.1. In June 2014 a Sensornet Oryx DTS was deployed on the fore reef of Dongsha Atoll in the South China Sea. Color contours shows nearbed water temperature on the fore reef for six hours on 05 June 2014. Strong temperature fronts indicate internal bores and swash on the inner kilometer of the shelf. The DTS measurements provide a unique and continuous view of high frequency and small-scale temperature variability within the reef ecosystem.

### *Hydrodynamic Controls on Habitat Heterogeneity*

One of the major challenges in understanding ecological processes is quantifying physical and biological patterns at appropriate scales. For example, rising sea surface temperatures threaten coral reefs on a global scale, but sub-meter scale patterns in temperature and flow fields can shape an individual coral colony’s thermal tolerance and influence recovery from an extreme thermal event [10]. During mass coral bleaching events there is commonly patchy survival of a small number of colonies and reef sections [11]. Much of the focus of thermal observations on coral reefs has been from satellite products at spatial scales larger than 4 km and temporal scales of weeks to months, but *in situ* observations reveal that extremely

different thermal microclimates can exist within a single reef flat (at spatial scales of 100s of meters) and diurnal temperature fluctuations on reefs can be as large as seasonal ranges. *What are we missing when we assess the environmental conditions on coral reefs from large-scale remote sensing products?* There is a pressing need to examine environmental variables at the scale that is relevant to the organisms. At the Fluid Dynamics of Living Systems meeting, we presented observations from an instrument relatively new to oceanographic research, a Distributed Temperature Sensing system, which uses the backscattered spectrum of light within a fiber optic cable to measure water temperature along the cable as shown in Fig. 1.1. These novel measurements will allow us to characterize habitat heterogeneity on scales from hundreds of meters down to centimeters and will overlap with historical coral monitoring stations to link spatial scales of physical variability to biological gradients within the reef.

## 2. Multi-scale/physics Image-Based Hemodynamics Modeling by Shawn C. Shadden

Research on fluid mechanics originated in considerable part from investigations of blood



flow. Indeed, the modern formulation of fluid mechanics set forth by Daniel Bernoulli, Leonhard Euler, and others was guided by investigations of flow in tubes [12,13]. While quasi-1D theories of fluid flow in tubes dominated theoretical and numerical investigations of blood flow for centuries, modern computing has enabled the investigation of local, 3D blood flow mechanics to understand the distribution of velocity, pressure and wall shear stress (WSS) at bends, bifurcations, aneurysms, stenoses, anastomoses, and other geometric transitions. Concomitantly, local disruptions in blood flow are known to be fundamental to the causes and consequences of most cardiovascular diseases and complications. Thus, a precise understanding of hemodynamics is key to improving the diagnosis and treatment of what are now the leading causes of death and disability worldwide.

Figure 2.1. CT angiography (left) is used to construct a 3D patient-specific arterial model (right).

The role of hemodynamics in any disease scenario is highly individualized. To address this challenge, medical imaging has paved the way for personalized computational modeling [14,15]. A typical example is to utilize 3D angiographic data obtained from CT or MRI to construct a geometric model of a portion of the vascular anatomy (Figure 2.1). The geometric

model is then discretized into a computational domain to simulate blood flow. Hemodynamic conditions commonly associated with disease localization and device complications occur primarily in larger vessels ( $>1\text{mm}$ ). In such regions, blood can be modeled as a homogeneous fluid and its mechanics can be simulated using computational fluid dynamics (CFD), subject to appropriate boundary conditions and constitutive relations. In addition to providing geometric boundary conditions, some imaging modalities can also provide fluid mechanic boundary conditions [16], vessel tissue properties [17], etc. The use of medical imaging to drive physics-based models is a budding field, with comprehensive open-source software now available to support such analyses (<http://simvascular.org>).

Image-based CFD chiefly provides highly resolved velocity and pressure data that can be used to better understand hemodynamic forces and transport processes. While the pathophysiology of any cardiovascular disease is multifaceted, computations of velocity and pressure alone can have significant impact in improving healthcare. As examples, image-based CFD of energy and flow distribution recently led to a novel redesign of the Fontan procedure (a surgery to reroute blood in patients with congenital heart defects) [18]; and the company HeartFlow has recently established the first routine use of image-based CFD in the clinical setting—to compute the pressure drop across a coronary stenosis for evaluating the need for treatment [19]. However, a number of challenges exist in broadening the impact of image-based hemodynamics modeling. Many of these challenges stem from the inherently complex coupling that exists between blood flow conditions and the physiologic responses these conditions elicit over disparate spatial and temporal scales *in vivo*. In the remainder of this section, we introduce some of our recent work presented at the Fluid Dynamics of Living Systems meeting involving “multi-scale/physics” applications of image-based hemodynamics modeling.

### Cerebrovascular reactivity

In all image-based hemodynamics models, one considers a truncated portion of the cardiovascular system and appropriate boundary conditions must be assigned. Significant progress has been made in accounting for upstream or downstream portions of the circulatory system by coupling the image-based model to reduced order models [20]. Often simple lumped parameter models are used; a common example is to specify a “resistance” at each outflow boundary, which fixes a ratio between flow rate and pressure. More sophisticated models are required, however, when the

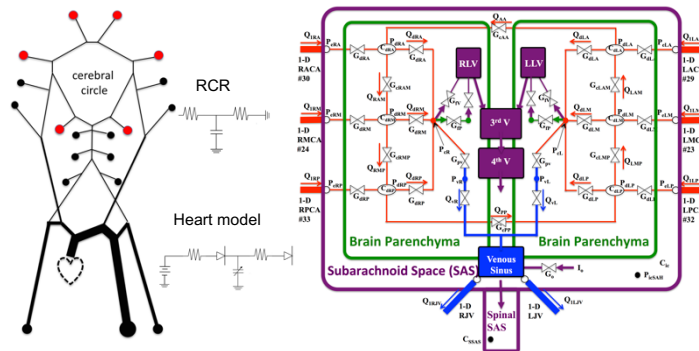


Figure 2.2. A comprehensive intracranial model (right) accounting for cerebral autoregulation, CSF and ICP dynamics, is coupled to a distributed model (left, coupled at red circles) to study pulse wave dynamics associated with cerebrovascular events. (Black circles for coupling to simpler RCR models.)

dynamic and reactive nature of the upstream or downstream portions becomes significant. This is paramount in the brain, where tight regulation of blood flow under various physiologic and pathologic conditions is required. We have recently worked to couple important features of cerebrovascular reactivity to image-based hemodynamics models (Figure 2.2). In Ryu et al. [21], we described the coupling of vascular flow models with dynamic lumped parameter networks that describe cerebral autoregulation, CO<sub>2</sub> reactivity, intracranial pressure (ICP), cerebrospinal fluid (CSF) dynamics, and cortical collateral blood flow. This framework has been validated against various clinical measurements including blood flow distribution, pulse waveforms of blood velocity and pressure, and the dynamic response of cerebral autoregulation during carotid compression, hyperventilation and CO<sub>2</sub> inhalation. Currently, this modeling is being used to improve monitoring (and our understanding) of various cerebrovascular events including ischemic stroke and vasospasm following sub-arachnoid hemorrhage.

### *Vascular growth and remodeling*

Most image-based hemodynamics computations simulate blood flow over a few seconds, whereas most cardiovascular diseases develop over months to years. To help understand the underpinnings between local hemodynamics and disease progression, methods to couple these disparate timescales are required. In Wu & Shadden [22] a computational framework to couple vascular growth and remodeling

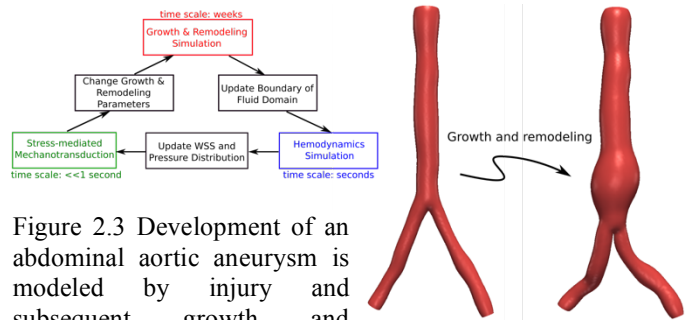


Figure 2.3 Development of an abdominal aortic aneurysm is modeled by injury and subsequent growth and remodeling simulation.

(VGR) with image-based hemodynamics simulation was presented in the context of aneurysm formation (Figure 2.3). Hyperelastic and anisotropic properties were considered for the vessel, and a constrained mixture model was used to represent constituent kinematics. The coupled simulation was divided into two time scales; one in which VGR is simulated to evolve the boundary of the fluid domain, and another in which fluid simulations in turn generate WSS and transmural pressure data that regulate VGR. Recent focus has been on multiscale coupling of stress-mediated cellular mechanotransduction pathways that cause remodeling in the vessel wall. By coupling these pathways, a more direct connection to the underlying biochemical and biomechanical regulatory responses are considered. This can enable potentially important macroscale behavior to be captured, such as intermittent aneurysm expansion, which is not otherwise well reproduced in current models. There has also been recent progress in extending previous VGR models for arteries to simulate adaptations veins [23], demonstrating that a gradual change in pressure loading for vein grafts may lead to more favorable growth responses compared to the abrupt pressure changes these grafts often confront.

## Thrombosis

Pathological clotting is the proximal cause of most heart attacks and strokes, and primary complication with most cardiovascular surgeries and devices. There is growing evidence and awareness regarding the importance local hemodynamic factors play in thrombus growth and structure, and increasing desire to couple image-based hemodynamics simulations to modeling thrombosis (or indirectly “thrombotic potential”). For example, recent work has demonstrated links between WSS parameters and thrombotic risk in aneurysms—both in the abdominal aorta [24] and coronary arteries [25]. Previous computational models of flow-mediated thrombogenesis have generally considered the transport and reaction of biochemical species

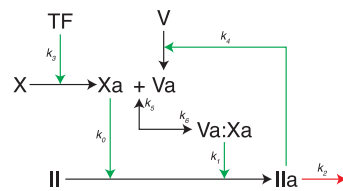


Figure 2.4 A reduced order model of the coagulation cascade has been shown to accurately reproduce thrombin generation, as well as other key species with reduced computational cost and complexity.

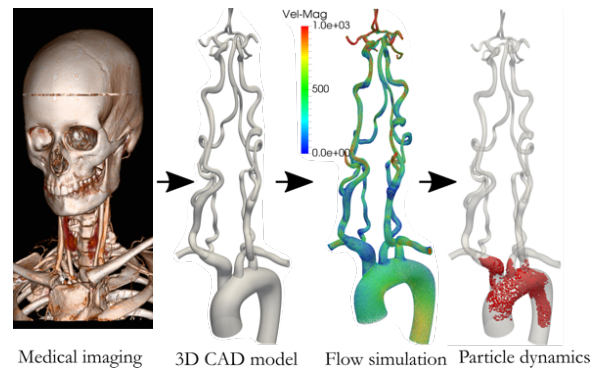
involved in the coagulation cascade. It is difficult to properly resolve such chemical transport problems in arterial flows however, due to the high Schmidt numbers and thin concentration boundary layers. There is also a disparity of time scales; the coagulation cascade occurs on the order of minutes while transport problems require time steps on order of a millisecond. These disparities lead to significant computational difficulties [26]. Moreover, common coagulation cascade models track dozens of species governed by largely unknown reaction rate constants. Coupling large vessel hemodynamics with mechanisms for thrombogenesis requires some reduction of the underlying physical models.

We have developed various methods to simplify the coagulation problem to enable its application to 3D image-based geometries. First, we have introduced an approach to reduce the order of a coagulation model through optimization techniques so that fewer species need to be tracked to capture the most relevant kinetics (Figure 2.4). These models reduce computational cost, and are easier to parameterize, however the latter remains a challenge in practical applications. We have also developed a framework [26] to reduce the high Schmidt number transport problem in large artery flows to surface transport equations on the vessel wall. The ability of this reduced order transport model to predict thrombogenic potential has been demonstrated by comparing to results from the (very costly) full 3D transport equations. While the modeling above considers a continuum-based approach by tracking the transport and reaction of biochemical species involved in the coagulation cascade, we believe there is also strong promise in multiscale [27] or systems biology [28] approaches, particularly in consideration of modeling of thrombus growth or fragmentation.

## Embolus transport

The coupling of blood and particle dynamics in cardiovascular flows has many important applications in disease and treatment scenarios. One of our focuses has been to better understand how the location, size or density of emboli (traveling thrombotic mass or intravascular debris) originating from the heart or aorta might determine stroke location and risk. We have recently demonstrated that propensity for cardio and aortogenic emboli to be transported to the carotid

and vertebral arteries supplying the head varies markedly from expectations based on blood distribution [29]. Moreover, it has been found that a patient’s aortic anatomy, and embolus origin for aortogenic emboli, significantly influence the probability of an embolus reaching the head. These factors indicate important mechanisms underlying embolic stroke etiology, and knowing or controlling for these may improve therapeutics to reduce embolic stroke risk, identify locations to avoid during endovascular procedures, or aid in prospective or retrospective evaluations of a particular patient.



We have also explored more fundamental aspects of modeling of fluid-particle interaction within image-based hemodynamics simulations [30]. Particle dynamics can be determined by the blood flow (and vessel wall), by either neglecting or accounting for the particle’s influence on the blood (or vessel wall)—leading to one and two-way coupling strategies respectively. Even for one-way coupled simulations, there are a number of choices on “force terms” to consider (lift, drag, buoyancy, unsteady effects, etc.). Our recent investigations have compared the magnitude of these forces in image-based hemodynamics simulations. Fluid acceleration and added mass forces were found to be dominant, however lift forces, although small, were important for example in pulling particles from the vessel wall. Two-way fluid-particle simulations are the gold standard, but far more costly, hence we have compared one- and two-way coupled simulations to determine the extent over which one-way coupling is justified in common vascular flow scenarios. We observed that for small to moderate particle sizes (relative to vessel diameters), particle distribution trends were similar between one and two way coupling schemes, yet this similarity breaks down once particle size increases. Motivated by the ability to model the dynamics of particles of occlusive diameters, and the aggregation of discrete elements at injury sites (thrombosis), our ongoing work has also focused on efficient fluid-solid interaction for fully-resolved fluid-particle simulations to enable such explorations.

### 3. Blood occlusions in the microcirculation by Thierry Savin

The microcirculation is the terminal network of blood vessels in organs, which distributes blood within the tissue for metabolic exchanges. It is composed of arterioles, capillaries and venules, and has a structure that also contributes to the regulation of blood pressure, vascular flow, and temperature. The microvascular network plays an important role in keeping tissues healthy, but it is also central in certain pathological conditions such as anemia or tumor-induced angiogenesis [31].

In the human microcirculation, the vessels’ diameters range from  $\sim 3 \mu\text{m}$  for the capillaries, to  $\sim 200 \mu\text{m}$  for the arterioles and venules. In comparison, the size of the red blood cells ( $8 \mu\text{m} \times$



3  $\mu\text{m}$  discocytes) or of the leukocytes ( $\sim 10\mu\text{m}$  for spheroidal neutrophils) are similar to the microvascular conduits: on the one hand, blood cells must reversibly deform to travel through the capillaries (possibly improving the metabolic exchanges); on the other hand, in the lumen of arterioles or venules, only 10-100 cells can be fitted in the cross-section.

This similarity of length scales, between the tube and the constituents of the suspension flowing through it, limits the use of continuum models when describing microcirculating blood. Neither its particulate nature, nor the interactions between its constituents or their individual mechanics, can indeed be ignored to explain observations such as the Fåhræus-Lindqvist effect (decrease of blood's apparent viscosity with decreasing tube diameter), blood's shear-thinning, or platelets and leukocytes' margination [31,32].

The geometry of the microvascular network also influences the integrated flow properties of the circulating blood. The angioarchitecture of the microcirculation has been measured in several organs. It exhibits a large array of geometries, fractal tree-like or abundant in loops, to meet the specific needs of each organ. Numbers of feeding arterioles and/or draining venules, densities of capillaries etc, are also varying factors in different organs. Nevertheless, certain hierarchical features are commonly found in the majority of vascular beds: a succession of cylindrical segments with decreasing diameter and length, and increasing number, as one moves from the arterioles to the capillaries; and symmetrically the same features are found on the side of the post-capillary venules [33].

Considerable efforts have been made to describe the blood flow in the microcirculation under physiological conditions. For example, at the single capillary level, detailed studies connect the shape and deformability of individual blood cell with their ability to flow through the narrow tubes [34]. More recently, various multiphase simulation frameworks were used to describe the motion of larger volumes of blood, in wider channels of some canonical geometry (straight or constricted channels, corners, Y-junction etc) [35,36]. At larger scales, theoretical studies are further attempting to link the optimum metabolic delivery, as permitted by the microvascular network, with its topology [37].

Yet, the microcirculation is not robust to certain pathological events. An archetypal example of possible failure is observed in sickle-cell disease (SCD). Affected patients carry a mutated hemoglobin that aggregates and polymerizes in the erythrocytes under hypoxic conditions. As a result, "sickled" red cells are stiffer and often exhibit abnormal shapes, both conditions preventing them to properly flow in the microcirculation upon oxygen release. Hindrance to their flow may also be increased by altered adhesive properties, and possibly accompanied by the secretion of other vasoactive substances. Ultimately these blockages can lead to painful and dangerous vaso-occlusive crises [38]. It is thus important to understand all the physical factors controlling the SCD clogging events. And if these blockages are local, the dynamics of their propagation throughout the entire microvascular network until its global failure also needs to be elucidated.

To do so, it seems judicious to adopt a bottom-up approach, and to first assess the conditions of flow arrest in the capillaries. Hence, several experimental studies have employed

microfluidic devices to measure single-cell obstructions of square capillaries produced via soft lithography [39,40]. The square cross-section is a significant departure from the biological reality, and makes theoretical approaches challenging. In a recent paper, we used a combination of experiments and theory to investigate how an impaired red blood cell can occlude capillary flow [41]. In contrast with the previous studies, we used a cylindrical conduit similar to the ones found in the microcirculation. This geometry allowed us to develop an elasto-hydrodynamic model of the occlusion, that accounts for the balance of membrane tension competing with the flow of the surrounding plasma at the onset of motion arrest (see Fig. 3.1). An extension of these experiments and models to SCD cells, which possibly occlude the flow through their bulk stiffness rather than their membrane tension, is currently being implemented.

In wider channels, *ex vivo* microfluidic models of arterioles and venules, injected with whole SCD blood, have been developed to reproduce vaso-occlusive events [42], quantify their severity [43], and to show enhanced cell depositions in the corners of bifurcations [44]. This latter recent study, paired with simulation results [45] and dedicated experiments [46], emphasizes the role of red cells' adhesion, with each other and with the endothelium, in the SCD vaso-occlusion

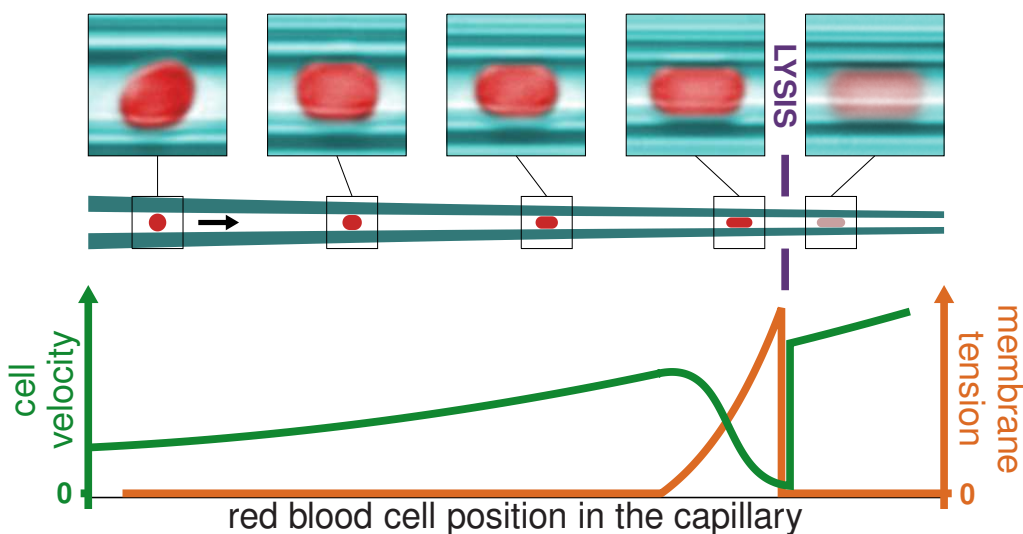


Figure 3.1: A pre-swollen red blood cell was pressure-driven and tracked in a narrowing cylindrical capillary. Near-occlusions were observed when the cell was squeezed to a level that required stretching its membrane to accommodate the confinement [41].

phenomenon. A semi-empirical, two-phase model was recently developed to describe the hydrodynamics of a vaso-occlusion [47]. However, the multi-cell dynamics determining the initiation and location of occlusive events largely remain unknown. And to our knowledge, vaso-occlusions in an entire network of channels have not been investigated.

There are still significant efforts to be made in experimental, theoretical and computational research to predict the formation of single-channel vaso-occlusions, from the interplay of blood cells' mechanics, adhesion, and geometry. Parallel to these biologically-motivated questions, there is a growing interest within the soft matter physics community to understand clogging of colloidal suspension flowing in microchannels and constrictions [48-50].

The tools and models developed to assess these may provide a promising avenue to study the probabilistic physics of channel vaso-occlusion. But a single occluded segment in the microcirculation is unlikely to be harmful, if the whole microvascular network remains unaffected. Thereby, the large-scale dynamics of global network failure should also be questioned. For example, it is known that the robustness of tree-like networks against failure is lower than the one of loop-structured transportation networks [51]. These different topologies are present in the body microcirculation [52], and such observations may be particularly relevant when tackling vaso-occlusions in entire microvascular networks.

#### 4. Fluid Dynamics of Disease Transmission and Health by Lydia Bourouiba

In humans or animals, infectious disease transmission might occur through direct contact with an infected individual, or it might occur through contact with or inhalation of smaller droplets containing pathogens. Populations (humans, animals, and plants) are complex multi-scale systems for which the mechanisms of small-scale pathogen transmission driving the large-scale population epidemic pattern remain poorly understood. While research in infectious diseases has made advances in understanding the cellular level microbiology of pathogen-host interactions, and the development of computational or mathematical models of spread of infectious disease at the population level, our understanding of the dynamics of disease transmission remains largely speculative.

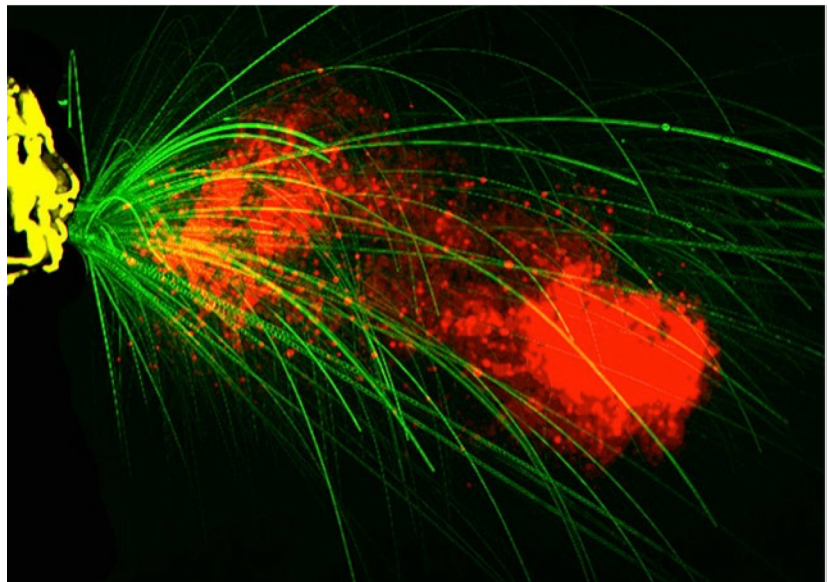


Figure 4.1: High-speed video imaging reveals two components of a sneeze: larger droplets whose ballistic trajectories (green) can extend up to 2 m from the sneezer (yellow), and a cloud of smaller droplets suspended in moist, warm gas (red) [57]. The tools of fluid dynamics allowed to discover the presence of the turbulent cloud via direct experimentation and using a mathematical model that the small droplets can be carried over much longer distances than previously thought (up to a factor of 200), allowing them to go further than the larger drops [58].

There are two principal groups of classical mathematical models of disease spread. First, compartmental models assume homogeneously mixed groups (classified as infectious, susceptible or exposed) interacting with each other through *contact* [53-56]. Second, network models represent populations, communities, hospitals, or individuals as vertices connected to the network by static or dynamic edges that model *contact* [56]. More recently, complexities such as

heterogeneity and individual variability have been explored thanks to the more powerful computers (e.g. individual-based models). Despite these advances, there remains a major gap in understanding fundamental processes of disease transmission from a mechanistic point of view. Filling this gap is essential to constructing a robust bottom-up multi-scale description of diseases epidemiology.

For example, the literature remains undecided as to the relative importance of long-range airborne transmission and short-range large droplet transmission for many diseases, including SARS, avian influenza, whooping cough, or Ebola [59-64]. In short, basic mechanisms governing the mode of acquisition and potential cross-infection of some deadly diseases remain very poorly understood. In fact, a critical gap in our mechanistic understanding of disease spread remains at the *mesoscopic scale*,

namely the transmission and contact modes between the individual host and the susceptible target. We simply do not know how pathogens actually transfer from one host to the next: *How do the dynamics of emission (shedding) of the pathogen from the host relate to the mode of transmission to the next host? How can the physical processes shaping the pathogen-host, the pathogen-environment, and the pathogen-susceptible interactions be linked to the spreading pattern at the population level?*

Fluid dynamics can play a critical role in understanding these steps at the *mesoscale* between large population scales and small molecular or microbiology scale. This becomes clear when one considers that peer-to-peer transmission and contact modes (regardless of the type of species or population) involve complex interactions between the pathogen and a fluid phase, such as droplets or multiphase clouds.

Consider how sneezing, coughing, and even breathing can transform an infectious patient into a potent source of bacteria and viruses, as most airborne bacteria and viruses reside in or on droplets. Recent visualizations of the fluid dynamics of the emissions from sneezes and coughs [67,68] enabled direct quantification of these processes [58] (e.g., Figs. 4.1 & 4.2a). A key finding of these experiments and their associated theoretical modeling and validation via the use of a physical fluid dynamics model is that the ejecta consists of a multiphase cloud in addition to the well understood ballistic large-droplet emissions. The combined clinical observation to fluid dynamics modeling led to a significant insight in the context of disease transmission: the multiphase cloud dynamics allows the small droplets to travel much farther (a factor of 200 in

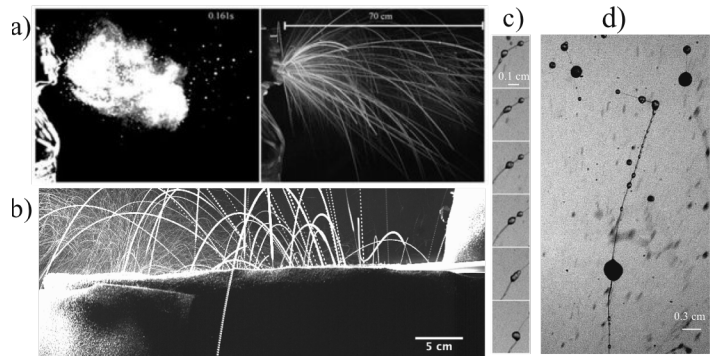


Figure 4.2: Fluid breakup and droplet creation in various systems contributing to disease transmission. a) respiratory ejections in the form of sneezes [58]. b) Toilet flushes generating contaminated droplets [65]. c-d) Detailed fragmentation process of mucosalivary fluid occurring during violent expirations and showing the importance of elasticity in the process of fragmentation [66].

range) than was previously appreciated for small-droplet ejections.

Although initial insights are starting to be gathered (e.g., Fig. 4.2c-d) [66], additional flow

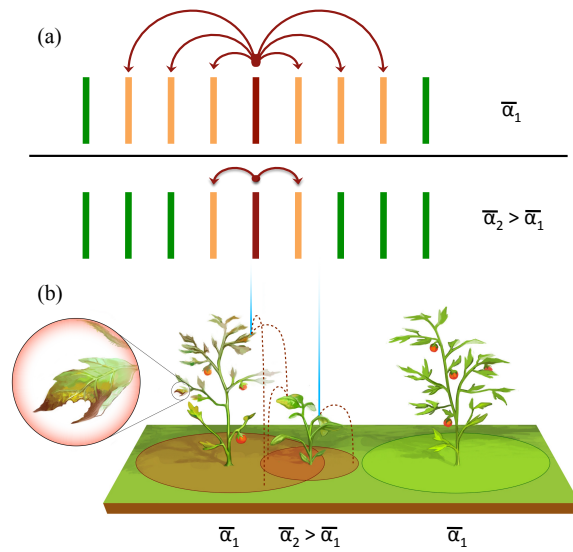


Figure 4.3: Understanding the mechanisms shaping the removal of pathogens from leaves and their ejection away from the leaves as a function of the fluid-structure interaction during rainfalls can lead to insights on the speed of disease spread (a) and the possible control strategies to be used for mitigation, such as alternating plants with complementary compliances as discussed in more details in Ref. [69].

the deposition of droplets and solid particles in the respiratory tract [e.g. 75-78], as arises during inhalation of pathogen-laden droplets. Here too, the influence of droplet size on its efficacy of transport within the airway networks remains poorly understood. *An improved model of the interaction of the turbulent flow in the airway system and suspended droplets and particles is another important frontier.*

Although most attempts at tackling the important problems above appear to have focused on the intersection of fluid dynamics and respiratory infectious diseases in humans, other problems at the intersection of fluid dynamics and infectious diseases require attention. Indeed, a rich class of fluid dynamics problems involving complex or turbulent flows can provide insight in transmission as it applies to coughs or sneezes in humans, but also in animal models, or in the larger context of chain of transmission in health facilities from plumes of infected individuals [58, 59, 66, 68, 73, 74, 80–84]. A class of fluid dynamics problems that involve fluid-structure interactions and also dispersal questions can shed light on important problems of contamination from infected produce or plants. These include rain-induced foliar disease transmission creating contaminated droplets that can deposit or spread via turbulent

visualization methods and experimental, numerical, and theoretical fluid dynamics tools are needed to rationalize the process of creation of the droplets emitted during violent expirations. Recent studies aimed at measuring the size distribution of droplets emitted by various respiratory functions, such as coughing or sneezing [70-72]. *However, for most diseases, no consensus on the drop distribution can be found. The discrepancy between reported data poses a basic impediment to the modeling of respiratory disease transmission, particularly in confined environments such as hospitals and airplanes [59,73,74].*

Inside the respiratory tract, previous studies focused on the transport of respiratory gases in the respiratory tract, including the role of flow curvature, secondary flows in bifurcating tubes, and the importance of heat and water exchange within the respiratory tract [75]. Another focus has been directed towards understanding

airflows to new plant hosts in agricultural fields (e.g., Fig. 4.3) [69, 85-87]. Finally, a rich class of problems involving interfacial flows can help shed light on waterborne pathogens or contaminants from waste waters that become suspended in the air in the form of droplets and droplet residues thanks to interfacial phenomena of destabilization and droplet creation as shown in Fig. 4.2b and Fig. 4.4

[65, 79, 88-90]. The range of problems cited in this section involve flows at various scales and of various complexities and can appear distinct; however, they share essential common features in their contribution to the chain of pathogen transmission between hosts of a population. A vision and focus on the development of the emerging field of fluid dynamics of disease transmission will be necessary to

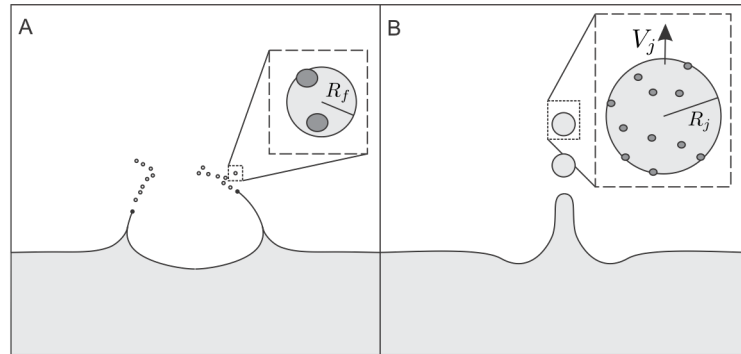


Figure 4.4: Illustration of the process of creation of contaminated droplets from the burst of bubbles of various sizes as they contribute to film drops (A) or jet drops (B). This process can be involved in a range of applications in contamination and infection from waste waters or waters containing water-borne pathogens [e.g., 79, 80]

tackle these important problems and root infectious disease prevention in the physical sciences that integrate clinical, physical, and mathematical tools to extract deep physical understanding and new principles governing infectious disease spread at the mesoscale where fluids are ubiquitous.

## 5. Respiratory flows in the deep pulmonary airways by Josué Sznitman

The past 25 years have witnessed a profound reshaping of our understanding of the respiratory fluid mechanics describing the acinar region of the lung. This region is made of hundreds of millions of sub-millimeter gas-exchange units (alveoli) characterized by low-Reynolds-number airflows. Historically, convective acinar flows first drew little attention since research was mostly driven by studies on gas (i.e. oxygen) transport and mixing [91]. Until the 1980s, low-Reynolds-number airflows in the distal regions of the lung were widely thought to be kinematically reversible with little flow-induced mixing [92]. In turn, for fine aerosols with little intrinsic motion (e.g., sedimentation, diffusion), the adopted view was that most inhaled particles would be exhaled without mixing with residual gas, leading to negligible deposition within the acinus.

This classic interpretation was, however, revisited after the seminal work of Heyder *et al.* (1988) who demonstrated with bolus studies in subjects that non-diffusing inhaled particles do in fact mix significantly with residual alveolar gas [93], such that convective mixing can occur in the lung periphery. This shift of paradigm combined with a rising concern to determine the fate of inhaled aerosols given their potential health risks or value as a therapeutic tool has led to a

resurgence of interest to unveil the complex nature of respiratory airflows in the pulmonary acinus.

Computational and experimental studies have contributed to improving our understanding of acinar flows and their intrinsic complexity over the past decade [94]. These have led to detailed characterizations of alveolar flow patterns (e.g. the existence of recirculating flows) and their implications for localized aerosol transport and deposition. Namely, it is acknowledged that inhaled particles ranging in size from 1 nm to 10  $\mu\text{m}$  are able to reach and deposit in the deep alveolated regions of the lungs [95]. While larger particles deposited in the acinus are overwhelmingly captured by sedimentation alone, a detailed knowledge of acinar fluid mechanics has helped illuminate our physical understanding of aerosol mixing of fine ( $<1 \mu\text{m}$ ) particles in the deep lungs.

To date, however, numerical studies have focused mainly on micron-sized particles whose deposition is governed foremost by sedimentation, thereby capturing only a small fraction of the broad range of aerosols accessing the acinar region. In particular, most studies have entirely discarded the local acinar transport dynamics of inhaled ultrafine particles ( $<100 \text{ nm}$ ) affected by diffusion and convection. Our efforts in this area, using computational fluid dynamics (CFD)

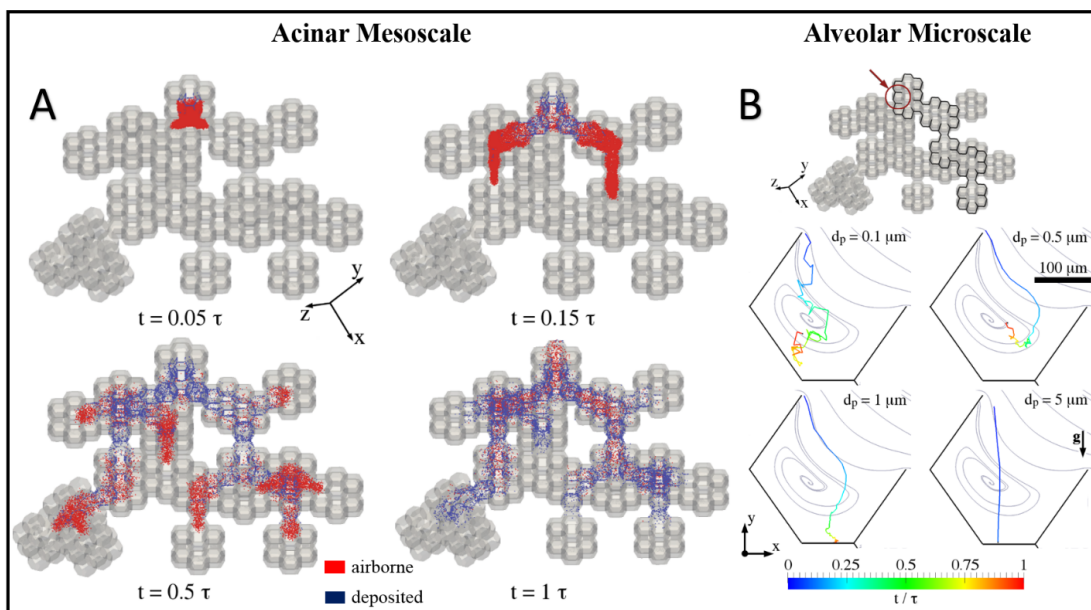


Figure 5.1: CFD simulations of acinar airflows and inhaled aerosol transport [96]. (A) Time-lapse sequence (1 breathing cycle  $\tau=3 \text{ s}$ ) of inhaled 100 nm diameter particles in a 3D space-filling acinar domain (airborne vs. deposited). (B) Time-resolved kinematics of individual aerosols in an alveolar cavity according to particle diameter.

simulations (Fig. 5.1), have aimed to reconcile our understanding of the physics governing the transport characteristics of particle sizes spanning three orders of magnitude (10 nm to 5  $\mu\text{m}$ ), covering all main transport mechanisms (i.e. diffusive, convective and gravitational aerosol motion). By characterizing the deposition patterns as a function of particle size across a multi-generational acinar network, our numerical models [96] underline how submicron particles reach deep into the acinar structure and are prone to deposit near alveolar openings. Our findings

highlight that a precise understanding of acinar aerosol transport, and ultrafine particles in particular, is contingent upon resolving the complex convective-diffusive mechanisms that determine their irreversible kinematics and local deposition sites.

Despite such progress, there remain still important gaps between the vast insight gathered through computational efforts relative to the few experimental validations and quantitative visualizations available on acinar flows. Importantly, there are no experimental visualization methods yet available to resolve particle dynamics in real lungs, in real time. As a result, experimental data on acinar deposition are generally unable to provide localized information of deposition sites but rely instead largely on regional deposition (e.g., alveolar region) obtained for example with inhaled boli techniques. Monitoring the transport of aerosols in air and the dynamics of their deposition in the alveolar tissue in particular, remains thus extremely challenging. To date, studying the movement of these particles *in vivo* using medical imaging modalities is limited [97], and thus quantitative assessments of aerosol transport in the acinus has remained somewhat a “black box.” Our group has recently developed a microfluidic platform, coined *acinus-on-chip*, which represents the first *in vitro* diagnostic tool enabling quantitative monitoring of the dynamics of inhaled aerosols directly at the acinar scales [98,99]. The life-size model lung allows, for the first time, direct and time-resolved observations of airborne particle trajectories and their patterns of deposition in alveoli. The innovative microfluidic model comprises a ramified network of minute air ducts approximately 100 microns wide, with small

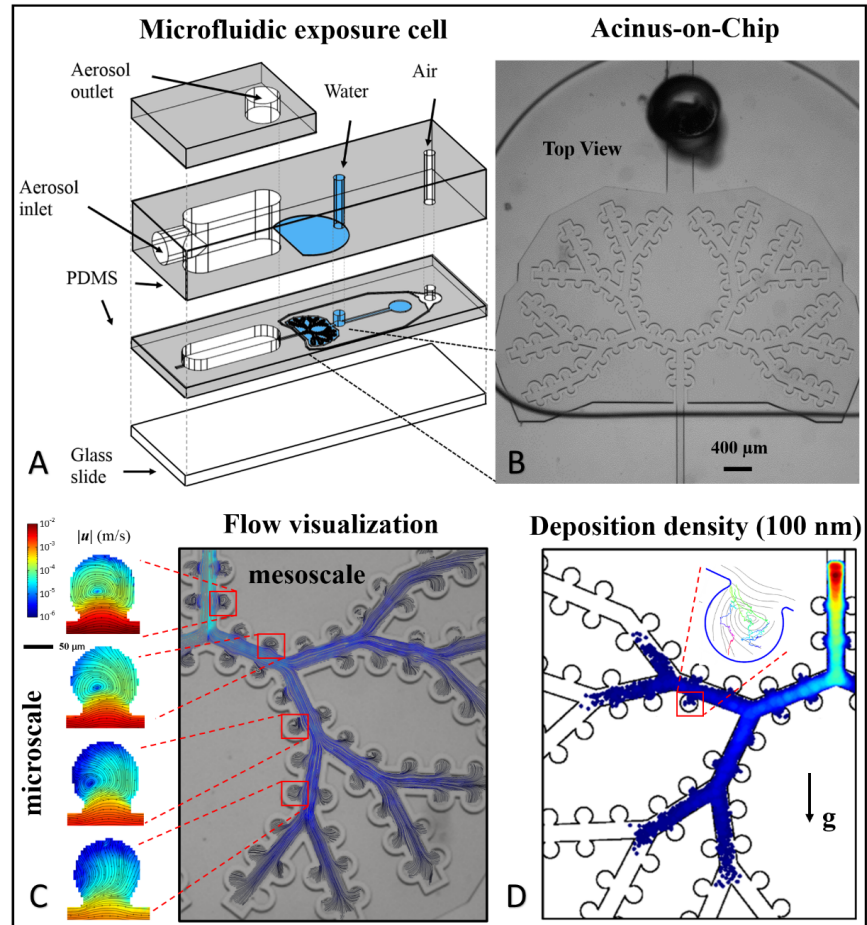


Figure 5.2: Microfluidic models of an *acinus-on-chip* [99]. (A) Multi-layered platform for inhaled aerosol exposure assays featuring (B) a multi-generation true-scale breathing acinar tree (moving walls). (C) Quantitative and time-resolved flow visualization at the meso- (tree) and microscale (alveoli). (D) Deposition patterns of inhaled nanoparticles (100 nm) following a breathing exposure assay (Inset: time-resolved aerosol trajectories in an alveolus).

microfluidic model comprises a ramified network of minute air ducts approximately 100 microns wide, with small



craters mimicking alveolar structures (Fig. 5.2). The walls of the system are actuated to expand and contract, mimicking physiological lung breathing. The model is expected to help give insight into the behavior of ‘bad’ inhaled particles (pollution) as well as ‘good’ therapeutic aerosols. Our *in vitro* model may reduce future needs for animal testing in the study of inhaled aerosols in the lungs.

Computational efforts will continue playing a critical, if not growing, role in addressing questions that may remain cumbersome for experiments, even with the advent of microfluidic platforms. For instance, there remains a dearth of knowledge on inhaled aerosol transport at mesoscale levels (e.g., within entire acini) and namely, on how to bridge our understanding of detailed acinar deposition in a single alveolus with predictions across the entire lung parenchyma. With increasing computational capabilities, these points will be addressed in the years to come.

## References

1. JA Kleypas & C Langdon, Coral reefs and changing seawater chemistry. Pp. 73-110 in *Coral Reefs and Climate Change: Science and Management*. JT Phinney, W Skirving, J Kleypas, and O. Hoegh-Guldberg, eds., American Geophysical Union, Washington, D.C., 2006
2. T Goreau, T McClanahan, R Hayes, & AL Strong, Conservation of coral reefs after the 1998 global bleaching event. *Conservation Biology*, **14** (1), 5-15 (2000).
3. O Hoegh-Gulberg, Climate change, coral bleaching and the future of the world’s coral reefs. *Mar. Freshwater Res.* **50**, 839–66 (1999).
4. SG Monismith, Hydrodynamics of coral reefs. *Annu. Rev. Fluid Mech.*, **39**, 37-55 (2007).
5. RE Britter, & SR Hanna, Flow and dispersion in urban areas. *Annu. Rev. Fluid Mech.* **35**, 469–96 (2003).
6. RJ Lowe, SG Monismith, & JL Falter, Oscillatory flow through submerged canopies: 1. Velocity structure. *J. Geophys. Res.* **110**, C10016 (2005).
7. RJ Lowe, U Shavit, JL Falter, JR Koseff, & SG Monismith, Modeling flow in coral communities with and without waves: a synthesis of porous media and canopy flow approaches. *Limnol. Oceanogr.* **53**, 2668-80 (2008).
8. MJ Atkinson, & RW Bilger, Effects of water velocity on phosphate uptake in coral reef-flat communities. *Limnol. Oceanogr.* **37**, 273–79 (1992).
9. SG Monismith, KA Davis, GG Shellenbarger, JL Hench, NJ Nidzieko, AE Santoro, MA Reidenbach, JH Rosman, R Holtzman, CS Martens, NL Lindquist, MW Southwell, & A Geninf, Flow effects on benthic grazing on phytoplankton by a Caribbean reef. *Limnol. Oceanogr.* **55**, 1881-92 (2010).
10. Pineda J, Starczak V, Tarrant A, Blythe J, Davis K, Farrar T, Berumen M, da Silva J. 2013. Two spatial scales in a bleaching event: Corals from the mildest and the most

- extreme thermal environments escape mortality. *Limnology and Oceanography* 58:1531-1545.
11. Guest JR, Baird AH, Maynard JA, Muttaqin E, Edwards AJ, Campbell SJ, Yewdall K, Affendi YA, Chou LM. 2012. Contrasting patterns of coral bleaching susceptibility in 2010 suggest an adaptive response to thermal stress. *PLoS ONE* 7:e33353.
  12. Bernoulli, *Hydrodynamica*, 1738.
  13. L Euler, *Principia pro motu sanguinis per arterias determinando*, (published posthumously 1862).
  14. CA Taylor, TJR Hughes, & CK Zarins, Computational Investigations in Vascular Disease, *Computers in Physics*, **10** (3), 224-232 (1996).
  15. DA Steinman, Image-based computational fluid dynamics modeling in realistic arterial geometries. *Ann. Biomed. Eng.*, **30** (4), 483-97 (2000).
  16. NM Wilson, FR Arko, & CA Taylor, Predicting changes in blood flow in patient-specific operative plans for treating aortoiliac occlusive disease, *Computer Aided Surgery*, **10** (4), 257-277 (2005).
  17. V Gurev, T Lee, J Constantino, H Arevalo, & NA Trayanova, Models of cardiac electromechanics based on individual hearts imaging data. *Biomech. Model. Mechanobiol.*, **10** (3), 295-306, 2011.
  18. AL Marsden, A Bernstein, VM Reddy, SC Shadden, RL Spilker, FP Chan, CA Taylor, & JA Feinstein, Evaluation of a novel Y-shaped extracardiac Fontan baffle using computational fluid dynamics. *J. Thorac Cardiovasc. Surg.*, **137** (2), 394-403 (2009).
  19. CA Taylor, TA Fonte, & JK Min, Computational fluid dynamics applied to cardiac computed tomography for noninvasive quantification of fractional flow reserve: Scientific basis. *J. Am. Coll. Cardiol.*, **61** (22), 2233-2241 (2013).
  20. K Lagana, G Dubini, F Migliavacca, R Pietrabissa, G Pennati, A Veneziani, & A Quarteroni, Multiscale modelling as a tool to prescribe realistic boundary conditions for the study of surgical procedures. *Biorheology* **39**(3-4), 359-364 (2002).
  21. J Ryu, X Hu, & SC Shadden, A coupled lumped-parameter and distributed network model for cerebral pulse-wave hemodynamics. *J. Biomech. Eng.*, **137**(10), 101009 (2015).
  22. J Wu, & SC Shadden, Coupled simulation of hemodynamics and vascular growth and remodeling in a subject-specific geometry. *Ann. Biomed. Eng.*, **43**(7), 1543-1554 (2015).
  23. Ramachandra AB, Sankaran S, Humphrey JD, Marsden AL, Computational simulation of the adaptive capacity of vein grafts in response to increased pressure, *Journal of Biomechanical Engineering*, 137, 031009, 2015.
  24. Arzani A, Suh GY, Dalman RL, Shadden SC, A longitudinal comparison of hemodynamics and intraluminal thrombus deposition in abdominal aortic aneurysms, *American Journal of Physiology- Heart and Circulatory Physiology*, **307**(12), H1786-H1795 (2014).
  25. D Sengupta, AM Kahn, O Shirinsky, G Lyskina, JC Burns, & AL Marsden, Thrombotic risk stratification using computational modeling in patients with coronary artery aneurysms following Kawasaki disease. *Biomechanics and Modeling in Mechanobiology*, **13**(6), 1261-1276 (2014).

26. KB Hansen, & SC Shadden, A reduced-dimensional model for near-wall transport in cardiovascular flows. *Biomech. Model. Mechanobiol.*, in press. DOI: 10.1007/s10237-015-0719-4 (2016).
27. Z Xu, N Chen, SC Shadden, JE Marsden, MM Kamocka, ED Rosen, & M Alber, Study of blood flow impact on growth of thrombi using a multiscale model. *Soft Matter*, **5** (4), 769-779 (2009).
28. JD Welsh, et al., A systems approach to hemostasis: 1, 2, 3. *Blood*, **124** (11), 1808-1831 (2014).
29. IA Carr, N Nemoto, RS Schwartz, & SC Shadden, Size-dependent predilections of cardiogenic embolic transport. *Am. J. Physiol. Heart Circ. Physiol.*, **305** (5), 732-739 (2013).
30. D Mukherjee, J Padilla J, & SC Shadden, Numerical investigation of fluid-particle interactions for embolic stroke, *Theor. Comp. Fluid Dyn.*, in press. DOI: 10.1007/s00162-015-0359-4 (2016).
31. AS Popel & PC Johnson, Microcirculation and Hemorheology, *Annu. Rev. Fluid Mech.* **37**, 43 (2005).
32. DA Fedosov, J Fornleitner, & G Gompper, Margination of white blood cells in microcapillary flow, *Phys. Rev. Lett.* **108**, 028104 (2012).
33. T Takahashi, *Microcirculation in Fractal Branching Networks* (Springer, Tokyo, 2014).
34. TW Secomb, R. Skalak, N. Özkaya, & J. F. Gross, Flow of axisymmetric red blood cells in narrow capillaries, *J. Fluid Mech.* **163**, 405 (1986).
35. JB Freund, Numerical simulation of flowing blood cells, *Annu. Rev. Fluid Mech.* **46**, 67 (2014).
36. K Lykov, X Li, H Lei, IV Pivkin, & GE Karniadakis, Inflow/Outflow Boundary Conditions for Particle-Based Blood Flow Simulations: Application to Arterial Bifurcations and Trees, *PLoS Comput. Biol.* **11**, e1004410 (2015).
37. B Moreau & B Mauroy, Murray's law revisited: Quémada's fluid model and fractal trees, *J. Rheol.* **59**, 1419 (2015).
38. GA Barabino, MO Platt, & DK Kaul, Sickle cell biomechanics, *Annu. Rev. Biomed. Eng.* **12**, 345 (2010).
39. JP Shelby, J White, K Ganesan, PK Rathod, & DT Chiu, A microfluidic model for single-cell capillary obstruction by Plasmodium falciparum-infected erythrocytes, *Proc. Natl. Acad. Sci. U.S.A.* **100**, 14618 (2003).
40. E Du, M Diez-Silva, GJ Kato, M Dao, & S Suresh, Kinetics of sickle cell biorheology and implications for painful vasoocclusive crisis, *Proc. Natl. Acad. Sci. U.S.A.* **112**, 1422 (2015).
41. T Savin, MM Bandi, & L Mahadevan, Pressure-driven occlusive flow of a confined red blood cell, *Soft Matter* **12**, 562 (2015).
42. JM Higgins, DT Eddington, SN Bhatia, & L Mahadevan, Sickle cell vasoocclusion and rescue in a microfluidic device, *Proc. Natl. Acad. Sci. U.S.A.* **104**, 20496 (2007).

43. DK Wood, A Soriano, L Mahadevan, JM Higgins, & SN Bhatia, A biophysical marker of severity in sickle cell disease, *Sci. Transl. Med.* **4**, 123ra26 (2012).
44. E Loiseau, G Massiera, S Mendez, PA Martinez, & M Abkarian, Microfluidic Study of Enhanced Deposition of Sickle Cells at Acute Corners, *Biophys. J.* **108**, 2623 (2015).
45. H Lei & GE Karniadakis, Probing vasoocclusion phenomena in sickle cell anemia via mesoscopic simulations, *Proc. Natl. Acad. Sci. U.S.A.* **110**, 11326 (2013).
46. Y Alapan, JA Little, & UA Gurkan, Heterogeneous Red Blood Cell Adhesion and Deformability in Sickle Cell Disease, *Sci. Rep.* **4**, 7173 (2014).
47. S Cohen & L Mahadevan, Hydrodynamics of hemostasis in sickle-cell disease, *Phys. Rev. Lett.* **110**, 138104 (2013).
48. HM Wyss, DL Blair, JF Morris, HA Stone, & DA Weitz, Mechanism for clogging of microchannels, *Phys. Rev. E* **74**, 061402 (2006).
49. KN Nordstrom, E Verneuil, PE Arratia, A Basu, Z Zhang, AG Yodh, JP Gollub, & DJ Durian, Microfluidic rheology of soft colloids above and below jamming, *Phys. Rev. Lett.* **105**, 175701 (2010).
50. A Sauret, EC Barney, A Perro, E Villermaux, HA Stone, & E Dressaire, Clogging by sieving in microchannels: Application to the detection of contaminants in colloidal suspensions, *Appl. Phys. Lett.* **105**, 074101 (2014).
51. E Katifori, GJ Szöllösi, & MO Magnasco, Damage and fluctuations induce loops in optimal transport networks, *Phys. Rev. Lett.* **104**, 048704 (2010).
52. P Blinder, PS Tsai, JP Kaufhold, PM Knutsen, H Suhl, & D Kleinfeld, The cortical angiome: an interconnected vascular network with noncolumnar patterns of blood flow, *Nat. Neurosci.* **16**, 889 (2013).
53. NF Britton. Essential Mathematical Biology. Springer Undergraduate Mathematics Series. Springer (2003).
54. AL Lloyd & RM May. Spatial heterogeneity in epidemic models. *J. Theor. Biol.*, **179** 1–11 (1996).
55. L Bourouiba, J Wu, S Newman, J Takekawa, T Natdorj, N Batbayar, CM Bishop, LA Hawkes, PJ Butler, & M Wikelski. Spatial dynamics of bar-headed geese migration in the context of h5n1. *J. R. Soc. Interface*, **7**, 1627–1639 (2010).
56. F Brauer, P van den Driessche, & J Wu. Mathematical Epidemiology. Lecture Notes in Mathematics: Mathematical Biosciences Subseries. Springer, (2008).
57. L Bourouiba. Image of the week: Anatomy of a sneeze. Howard Hughes Medical Institute, (2015).
58. L Bourouiba, E Dehandschoewercker, & JWM Bush. Violent expiratory events: on coughing and sneezing. *J. Fluid Mech.*, **745**, 537–563 (2014).
59. JW Tang, Y Li, I Eames, PKS Chan, & GL Ridgway. Factors involved in the aerosol transmission of infection and control of ventilation in healthcare premises. *J. Hospital Infection*, **64**, 100–114 (2006).
60. TP Weber & NI Stilianakis. Inactivation of influenza A virus in the environment and

- modes of transmission: A critical review. *J. Infections*, **57**, 361–373 (2008).
61. MT Osterholm, KA Moore, NS Kelley, LM Brosseau, G Wong, FA Murphy, CJ Peters, JW Leduc, PK Russell, M Van Herp, J Kapetshi, JT Muyembe, B Kebela Ilunga, JE Strong, A Grolla, A Wolz, B Kargbo, DK Kargbo, P Formenty, DA Sanders, & P Kobinger. Transmission of Ebola Viruses : What We Know and What We Do Not Know. *mBio*, **6**, 1–9 (2015).
  62. R Tellier. Aerosol transmission of influenza A virus: a review of new studies. *J. R. Soc. Interface*, **6**, S783–S790 (2009).
  63. RP Clarck & ML de Calcina-Goff. Some aspects of the airborne transmission of infection. *J. R. Soc. Interface*, **6** S767–S782 (2009).
  64. R Tellier. Review of Aerosol Transmission of Influenza A Virus. *Emerg Infect Dis*, **12** (11), 1657-1662 (2006).
  65. G Traverso, S. Laken, C-C Lu, R Maa, R Langer, & L Bourouiba. Fluid fragmentation from hospital toilets. American Physics Society - Division of Fluid Dynamics. Gallery of Fluid Motion, (2013).
  66. BE Scharfman, AH Techet, JWM Bush, & L Bourouiba. Visualization of sneeze ejecta: steps of fluid fragmentation leading to respiratory droplets. *Experiments in Fluids*, in press.
  67. GS Settles. Fluid mechanics and homeland security. *Annu. Rev. Fluid Mech.*, **38**, 87–110, (2006).
  68. L Bourouiba, E Dehandschoewercker, & JWM Bush. The fluid dynamics of coughing and sneezing. In Refereed proceedings of the International Society of Indoor Air Quality and Climate 10th Healthy Buildings Conference Brisbane. AU (2012).
  69. T Gilet & L Bourouiba. Fluid fragmentation shapes rain-induced foliar disease transmission. *J. R. Soc. Interface*, **12**, 20141092 (2015).
  70. RS Papineni & FS Rosenthal. The size distribution of droplets in the exhaled breath of healthy human subjects. *J. Aerosol Med.*, **10**, 105–116 (1997).
  71. S Yang, L. Gwm, CM Chen, CC Wu, & KP Yu. The size and concentration of droplets generated by coughing in human subjects. *J. Aerosol Med.*, **20**, 484–494 (2007).
  72. L Morawska, G Johnson, Z Ristovski, M Hargreaves, K Mengersen, S Corbett, C Chao, Y Li, & D. Katoshevski. Size distribution and sites of origin of droplets expelled from the human respiratory tract during expiratory activities. *J. Aerosol Sci.*, **40**, 256–269 (2009).
  73. JW Tang, I Eames, Y Li, YA Taha, P Wilson, G Bellingan, KN Ward, & J Breuer. Door-opening motion can potentially lead to a transient breakdown in negative-pressure isolation conditions: the importance of vorticity and buoyancy airflows. *J. Hospital Infection*, **61**, 283–286 (2005).
  74. I Eames, JW Tang, Y Li, & P Wilson. Airborne transmission of disease in hospitals. *J. R. Soc. Interface*, **6**, S697–S702 (2009).
  75. JB Grotberg. Pulmonary flow and transport phenomena. *Annu. Rev. Fluid Mech.*, **26**, 529–

571 (1994).

76. RB Schlesinger & M Lippmann. Particle deposition in the trachea: in vivo and in hollow casts. *Thorax*, **31**, 678–684 (1976).
77. W-I Li, M Perzl, J Heyder, R Langer, JD Brain, KH Englmeier, RW Niven, & DA Edwards. Aerodynamics and aerosol particle deaggregation phenomena in model oral-pharyngeal cavities. *J. Aerosol Sci.*, **27** (8), 1269–1286 (1996).
78. KW Stapleton, E Guentsch, MK Hoskinson, & WH Finlay. On the suitability of k-[var epsilon] turbulence modeling for aerosol deposition in the mouth and throat: a comparison with experiment. *J. Aerosol Sci.*, **31** (6), 739–749 (2000).
79. PLL Walls, JC Bird, & L Bourouiba. Moving with Bubbles: A Review of the Interactions between Bubbles and the Microorganisms that Surround them. *Integr. Comp. Biol.*, **54** (6), 1–12 (2014).
80. L Bourouiba & JWM Bush. Drops and Bubbles. Handbook of Environmental Fluid Dynamics Volume one: Overview and Fundamentals. Taylor & Francis Book Inc., (2013).
81. JW Tang, FRC Path, & GS Settles. Coughing and aerosols. *N. Engl. J. Med.*, **359**, e19 (2008).
82. JW Tang, TJ Liebner, BA Craven, & GS Settles. A schlieren optical study of the human cough with and without wearing masks for aerosol infection control. *J. R. Soc. Interface*, **6**, S727–S736 (2009).
83. JW Tang, CJ Noakes, PV Nielsen, I Eames, A Nicolle, Y Li, & GS Settles. Observing and quantifying airflows in the infection control of aerosol- and airborne-transmitted diseases: an overview of approaches. *J. Hospital Infection*, **77** (3), 213–22 (2011).
84. BA Craven & GS Settles. A Computational and Experimental Investigation of the Human Thermal Plume. *J. Fluids Engineering*, **128** (6), 1251 (2006).
85. T Gilet & L Bourouiba. Rain-induced Ejection of Pathogens from Leaves: Revisiting the Hypothesis of Splash-on-Film using High-speed Visualization. *Integr. Comp. Biol.*, **54** (6), 974–84 (2014).
86. DE Aylor. The role of intermittent wind in the dispersal of fungal pathogens. *Annu. Rev. Phytopathol.*, **28**, 73–92 (1990).
87. PE Waggoner & DE Aylor, Epidemiology: A Science of Patterns. *Ann. Rev. Phytopathol.*, **38**, 71–94 (2000).
88. L Bourouiba, DL Hu, & R Levy, Surface-Tension Phenomena in Organismal Biology: An Introduction to the Symposium. *Integr. Comp. Biol.*, **54**, 955–958 (2014).
89. DC Blanchard and LD Syzdek, Water-to-Air Transfer and Enrichment of Bacteria in Drops from Bursting Bubbles. *Appl. Environm. Microb.*, **43** (5), 1001–5, May (1982).
90. EC Martin, BC Parker, & JO Falkinham 3<sup>rd</sup>, Epidemiology of infection by nontuberculous mycobacteria. *Amer. Rev. Resp. Disease*, **136** (2), 344–348 (1987).
91. ER Weibel, B Sapoval, & M Filoche, Design of peripheral airways for efficient gas exchange. *Respir. Physiol. Neurobiol.* **148**, 3–21 (2005).

92. TJ Pedley, Pulmonary fluid dynamics. *Annu. Rev. fluid Mech.* **9**, 229–274 (1977).
93. J Heyder, JD Blanchard, HA Feldman, & JD Brain, Convective mixing in human respiratory tract : estimates with aerosol boli. *J. Appl. Physiol.* **64**, 1273–1278 (1988).
94. J Sznitman, Respiratory microflows in the pulmonary acinus. *J. Biomech.* **46**, 284–98 (2013).
95. W Stahlhofen, G Rudolf, & AC James, Intercomparison of Experimental Regional Aerosol Deposition Data. *J. Aerosol Med.*, **2**, 285–308 (1989).
96. P Hofemeier, & J Sznitman, Revisiting pulmonary acinar particle transport: convection, sedimentation, diffusion and their interplay. *J. Appl. Physiol.* **118**, 1375–1385 (2015).
97. J Conway, Lung imaging - two dimensional gamma scintigraphy, SPECT, CT and PET. *Adv. Drug Deliv. Rev.* **64**, 357–68 (2012).
98. R Fishler, MK Mulligan, & J Sznitman, Acinus-on-a-chip: a microfluidic platform for pulmonary acinar flows. *J. Biomech.* **46**, 2817–23 (2013).
99. R Fishler, P Hofemeier, Y Etzion, Y Dubowski, & J Sznitman, Particle dynamics and deposition in true-scale pulmonary acinar models. *Sci. Rep.* **5**, 14071 (2015).